# Novel Scaling Laws for the Langmuir-Blodgett Solutions in Cylindrical and Spherical Diodes

Y. B. Zhu,[1,4] P. Zhang,[2] A. Valfells,[3] L. K. Ang,[1,4,*] and Y. Y. Lau[2]

[1]*Engineering Product Development, Singapore University of Technology and Design, Singapore 138682, Singapore*
[2]*Department of Nuclear Engineering and Radiological Sciences, University of Michigan, Ann Arbor, Michigan 48109-2104, USA*
[3]*School of Science and Engineering, Reykjavik University, Menntavegi 1, 101 Reykjavk, Iceland*
[4]*School of Electrical and Electronic Engineering, Nanyang Technological University, Singapore 639798, Singapore*

(Received 31 January 2013; published 28 June 2013)

It is found that the Langmuir-Blodgett solutions for the space charge limited current density, for both cylindrical and spherical diodes, may be approximated by $J_{\rm app} = (4/9)\varepsilon_0\sqrt{(2e/m)}(E_c^{3/2}/\sqrt{D})$ over a wide range of parameters, where $E_c$ is the surface electric field on the cathode of the *vacuum* diode and $D$ is the anode-cathode spacing. This dependence is valid whether $R_a/R_c$ is greater than or less than unity, where $R_a$ and $R_c$ are, respectively, the anode and cathode radius. Minor empirical corrections to the above scaling yield fitting formulas that are accurate to within 5% for $3 \times 10^{-5} < R_c/R_a < 500$. An explanation of this scaling is given. An accurate transit time model yields the Langmuir-Blodgett solutions even in the Coulomb blockade regime for a nanogap, where the electron number may be in the single digits, and the transit time frequency is in the THz range.

DOI: 10.1103/PhysRevLett.110.265007 PACS numbers: 52.59.Sa, 85.30.Fg, 85.45.−w

Space-charge-limited electron flow describes the maximum current density allowed for steady-state electron beam transport across a diode. It is central to the studies of high current diodes, high power microwave sources, vacuum microelectronics, and sheath physics in plasma processing, etc. It is also of interest to the contemporary studies of the nanogap and nanodiode. For a one-dimensional (1D) planar diode with a gap spacing $D$ and gap voltage $V_g$, the maximum steady-state current density is governed by the 1D Child-Langmuir (CL) law [1,2],

$$J_{\rm CL} = \frac{4}{9}\varepsilon_0\sqrt{\frac{2e}{m}}\frac{V_g^{3/2}}{D^2}, \tag{1}$$

where $e$ and $m$ are, respectively, the charge and mass of the electron, and $\varepsilon_0$ is the permittivity of free space. There are extensions to this 1D classical CL law to multidimensions [3–8], to the quantum regime [9–13], and to ultrafast processes [14,15]. There are also related studies on the cylindrical diode [16,17], THz sources [18], time-dependent models [19–21], Coulomb blockade [22], and 2D electromagnetic effects [23].

The CL current may be simply approximated by $I = Q/T$, where $Q = CV_g$ is the total bound surface charge on the cathode, $C$ is the diode capacitance, and $T$ is the transit time of an electron to cross the gap subjected only to the vacuum field [24]. This capacitance model, or transit time model, yields a current density also given by Eq. (1) for the planar gap, except the numerical factor $4/9$ is replaced by $1/2$, thus committing an error of only 12.5% [24]. That is, we need to multiply the current density obtained from the transit time model by the numerical factor $8/9$ to obtain the correct CL law in a planar gap. Because of its simplicity and accuracy, this capacitance or transit time model is of great utility to study a short pulse diode [14], and more recently the quantum regime [13].

It is tempting to apply the transit time model to the cylindrical and spherical geometries that were treated by Langmuir and Blodgett (LB) [25,26]. LB obtained the space-charge-limited current density on the cathode of a cylindrical diode [25],

$$J_{\rm LB} = \frac{4}{9}\varepsilon_0\sqrt{\frac{2e}{m}}\frac{V_g^{3/2}}{R_a R_c \beta^2}, \tag{2}$$

where $\beta$ is a function of $R_a/R_c$ which is tabulated numerically, and $R_a$ and $R_c$ are the radius of anode and cathode, respectively. For the spherical diode, LB expressed $\beta^2$ as $(R_c/R_a)\alpha^2$ and tabulated $\alpha$ numerically as a function of $R_a/R_c$ [26]. Figures 1 and 2 show, respectively, the LB solution [Eq. (2)] for the cylindrical and spherical diode, over a wide range of $R_c/R_a (3 \times 10^{-5} < R_c/R_a < 500)$. In these figures, we set $V_g = 1$ V, and the inner radius of the diode at 1 cm, whether it be the anode or cathode radius. It is clear from Eq. (2) that, once the gap voltage and the inner radius are fixed, $J_{\rm LB}$ depends only on the radius ratio $R_c/R_a$, and $J_{\rm LB}$ at other values of gap voltage and inner radius may be obtained accordingly.

The LB solutions are not easy to obtain, and it is highly desirable to derive an accurate approximation with an adequate physical picture describing their underlying scalings. With the emergence of nanoparticles and nanotubes, scaling laws in these geometries would be of interest. To our knowledge, there is no simple analytical approximation for the LB solution [Eq. (2)], except for a recent model [17] that approximately solved the Poisson equation for a cylindrical diode. We shall comment on Ref. [17] later in this Letter.

 

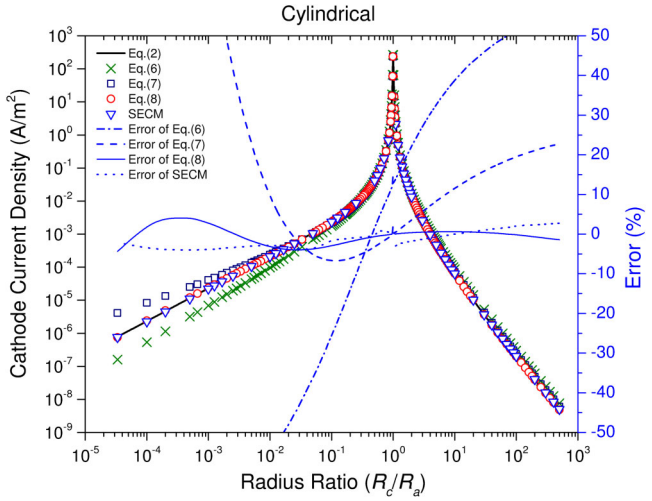


FIG. 1 (color online). Comparison between the LB law, Eq. (2), (solid line) and its various approximations for a cylindrical diode over a wide range of $R_c/R_a$. The inner radius either $R_c$ or $R_a$ is 1 cm. The applied voltage is $V_g = 1$ V. Symbols represent the approximate expressions: crosses for Eq. (6), the transit time model; squares for Eq. (7); circles for Eq. (8); and triangles for the SECM. Also plotted is the error in the approximate formulas compared with the LB law.

Since the transit time model depends only on the vacuum field solution in the diode, we summarize the magnitude of the vacuum electric field $E(r)$ and its potential function $V(r)$ in the cylindrical and spherical diode,

$$E(r) = E_c R_c/r, \qquad V(r) = E_c R_c |\ln(r/R_c)|,$$
$$V_g = E_c R_c |\ln(R_a/R_c)|, \qquad \text{cylindrical} \tag{3}$$

$$E(r) = E_c (R_c/r)^2, \qquad V(r) = E_c R_c |R_c/r - 1|,$$
$$V_g = E_c R_c D/R_a, \qquad \text{spherical} \tag{4}$$

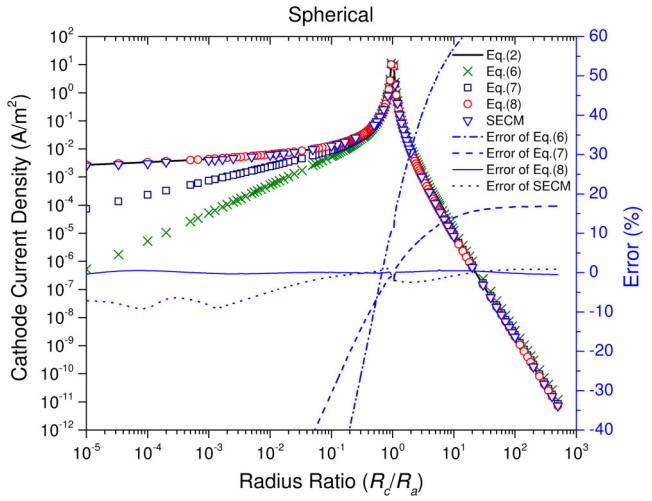


FIG. 2 (color online). Same as in Fig. 1, except for a spherical diode.

whether $R_c > R_a$ or $R_c < R_a$. In Eqs. (3) and (4), $D = |R_a - R_c|$ is the gap separation, and the last expressions give the relation between the gap voltage $V_g$ and the magnitude of the vacuum electric field $E_c$ on the cathode surface. In the planar limit, both Eqs. (3) and (4) give $V_g = E_c \times D$, whereas the LB law, Eq. (2), reduces to the CL law, Eq. (1).

In the transit time model [24], an electron is subjected to the vacuum fields, Eqs. (3) and (4), and the time of flight of an electron across the gap ($T$) is given by

$$T = \left| \int_{R_c}^{R_a} \frac{dr}{v(r)} \right| = \sqrt{\frac{m}{2e}} \left| \int_{R_c}^{R_a} \frac{dr}{\sqrt{V(r)}} \right|, \tag{5}$$

where $V(r)$ is given by Eq. (3) or Eq. (4). In writing Eq. (5), we have used the energy conservation relation $mv^2/2 = eV(r)$. The transit time model then yields, for both cylindrical and spherical diodes,

$$J_{\text{transit-time}} = \frac{\varepsilon_0 E_c}{T}, \tag{6}$$

because the surface charge density on the cathode of a *vacuum* diode is equal to $\varepsilon_0 E_c$ by Gauss's law.

The transit-time model, Eq. (6), is presented in Figs. 1 and 2 to compare with the exact LB solutions, Eq. (2). The percentage error in the transit-time model is shown by the dashed-dotted curves in Figs. 1 and 2. Over much of the ranges of $R_c/R_a$ that were considered by LB, these percentage errors greatly exceed the 12.5% error that is incurred in the transit-time model for the planar diode [24].

The poor agreement between the transit time model and the exact LB solutions for the cylindrical and spherical diodes, which was also noted independently by Carter [27], prompted us to look for a more accurate approximation to the LB solutions, Eq. (2). We find that, over a fairly large range of $R_c/R_a$, the LB solutions may be approximated by

$$J_{\text{app}} = \frac{4}{9}\varepsilon_0 \sqrt{\frac{2e}{m}} \frac{E_c^{3/2}}{\sqrt{D}}, \qquad \text{cylindrical or spherical,} \tag{7}$$

where $E_c$ is the cathode surface electric field of a vacuum diode that is given by Eqs. (3) and (4) and $D$ is the gap spacing, irrespective of whether the cathode is inside or outside the anode. Note the very different new scaling, Eq. (7), from Eq. (2). Note also that Eq. (7) becomes the exact CL solution, Eq. (1), in a planar cathode, for which $E_c = V_g/D$.

The approximate solution, Eq. (7), is also presented in Figs. 1 and 2. Its percentage error in comparison with the exact LB model, Eq. (2), is shown by the dashed curves in Figs. 1 and 2. These figures show that Eq. (7) is accurate to within 30%, for $0.1 < R_c/R_a < 500$, whether the diode is cylindrical or spherical. It is far more accurate than the transit time model, Eq. (6), and over a much wider range of $R_c/R_a$.

Before we give a physical interpretation of Eq. (7), we present an empirical correction to Eq. (7) that fits the exact LB solution over the large ranges of $R_c/R_a$ considered by LB [25,26],

$$J_{\text{app}} = \frac{4}{9}\varepsilon_0\sqrt{\frac{2e}{m}}\frac{E_c^{3/2}}{\sqrt{D}}[1 + F(R_c/R_a)], \quad \text{cylindrical or spherical.} \tag{8}$$

Here, the correction factor $F$ within the range $3 \times 10^{-5} < R_c/R_a < 500$ is given, for a cylindrical diode, by

$$F\left(\frac{R_c}{R_a}\right) = \exp\left[\frac{(s - s_0)(7s + 23)(8s - 417)}{143742}\right] - 1 \tag{9}$$

and, for a spherical diode, by

$$F\left(\frac{R_c}{R_a}\right) = \exp\left[\frac{(s - s_0)(9s - 37)(4s + 143)}{42092}\right] - 1, \tag{10}$$

where $s = \ln[\ln(1 + R_c/R_a)]$ and $s_0 = \ln[\ln(2)]$. Note that $F = 0$ when $R_c/R_a = 1$, as expected.

The improved approximate solution, Eq. (8), is also presented in Figs. 1 and 2. Its percentage errors in comparison with the exact LB model, Eq. (2), are shown by the thin, solid curves in Figs. 1 and 2. These figures show that Eq. (8) is accurate to within 5% for $3 \times 10^{-5} < R_c/R_a < 500$, whether the diode is cylindrical or spherical. Note from Figs. 1 and 2 that, over this range of $R_c/R_a$, the LB solution varies over many orders of magnitude.

The value of the correction factor $F$ in Eq. (8) is small compared with unity when the cathode is on the outside. That is, Eq. (7) provides the dominant scaling if the cathode is closer to the planar geometry relative to the anode surface. On the other hand, if the cathode is inside and the anode is outside at a large distance ($R_c/R_a \ll 1$), the cathode surface is poorly approximated by a planar surface and the correction factor $F$ is of order unity or larger. Thus, the dominant scaling, Eq. (7), may be deduced by concentrating at the close proximity of the cathode surface, where the local curvature effects of the cathode can be neglected, and the anode would play a secondary role.

To qualitatively derive Eq. (7), consider a sheet of charge leaving the cathode of a *vacuum* diode. If all the bound charge on the cathode leaves then naturally the electric field directly in front of the cathode becomes zero, and the space-charge-limited condition applies. This charge sheet will then be accelerated by the vacuum field, $E_c$, that is set up by the anode voltage, at least initially. Applying the transit time argument to this charge sheet, as we did in our earlier paper on a charge sheet [14], we note that the major portion of the transit time is spent in the immediate neighborhood of the cathode surface, where the electrostatic potential may then be approximated by, $V(r) \cong |E_c(r - R_c)|$. Using this $V(r)$ in Eq. (5), we obtain the approximate transit time, $T_{\text{app}} = 2(mD/2eE_c)^{1/2}$. Using this approximate transit time in Eq. (6), we obtain the approximate current density, $J_{\text{app}} = (8/9)\varepsilon_0 E_c/T_{\text{app}}$, which is Eq. (7). The factor of (8/9) is inserted here so that the transit time formulation is identical to the CL law, Eq. (1), in the limit of a planar diode [24]. The scaling law, Eq. (7), when applied to the cylindrical diode, is the same as the approximate formula published by Chen *et al.* [17] who also examined the region close to the cathode surface. Chen did not consider the spherical diode, nor did he write his approximate solution in the general form of Eq. (7). In fact, in his derivation [17], there was the ambiguity in the replacement of the differential distance ($\Delta r$) with the gap separation $D$ when he derived his Eq. (16) from his Eq. (15).

The use of the vacuum field ignores the space charge effect that is empirically modeled by the correction factor $F$ in Eq. (8). To correctly include the space charge effect in the transit time model, we inject a single electron (in the form of an infinitesimally thin cylindrical or spherical shell) into the diode, one at a time [22]. At time $t = 0$, there are $N$ electrons located on the cathode, ready to be injected into the gap, and the order of injection is labeled by $n = 1, 2, \ldots, N$. An electron (shell) is injected into the gap only if the total electric field acting on it would initiate an acceleration toward the anode. For the first electron to be injected, the imposed gap voltage must exceed a threshold voltage, $V_{\text{th}} = e/2C$, where $C$ is the capacitance in the cylindrical or spherical diode. (This threshold voltage leads to Coulomb blockade in the single-electron regime.) The radial position of the $n$th electron shell, denoted as $r_n(t)$, is computed from the total force acting on it. The Ramo-Shockley theorem [28,29] yields the instantaneous current through the diode, $I(t) = dq(t)/dt$, where $q(t)$ is the induced charge $q(t)$ on the capacitor. For a cylindrical diode with $R_c < R_a$, $q(t)$ is given in terms of $r_n(t)$ by $q(t) = CV_g + [e/\ln(R_a/R_c)]\sum_{n=1}^{N}\ln[r_n(t)/R_c]$. The time-average current for the $N$ injected electrons is equal to $\langle I\rangle = eN/t_N$, where $t_N$ is the total time measured from the first electron $n = 1$ when it is injected from the cathode and the time when the $N$th electron arrives at the anode.

The current density on the cathode, calculated from $\langle I\rangle = eN/t_N$ is also presented in Figs. 1 and 2, designated as "single electron capacitor model" (SECM). Its percentage errors in comparison with the exact LB model, Eq. (2), are shown by the dotted curves in Figs. 1 and 2. These figures show that SECM is accurate to within 10% in the entire studied range of $R_c/R_a$, an acceptable result in these particle-in-cell-like simulations.

We shall next show that the LB law also applies to the Coulomb blockade regime, i.e., to low numbers of $N$. In Fig. 3, we show the normalized $\langle I(t)\rangle$ relative to the LB value (solid line) for $R_c = 100$ nm, $D = R_a - R_c = 100$ nm, and $N = 50$ with $E_c/E_{\text{th}} = 1.02$ to 3.5. The higher than LB value shown in the range of $1 < E_c/E_{\text{th}} < 2$, due to the Coulomb blockade effect [22], was recently

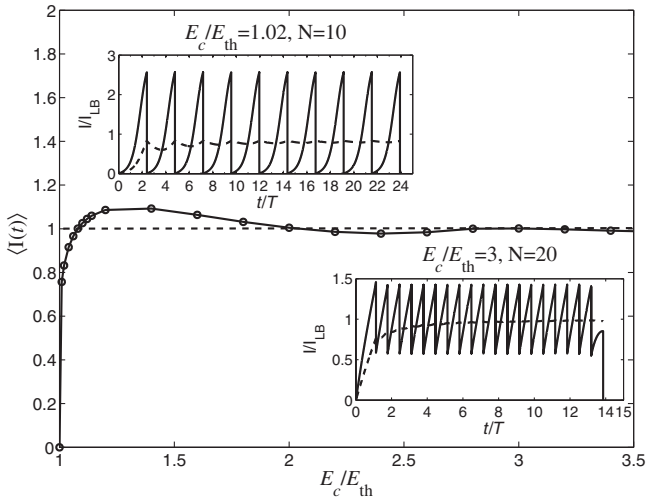


FIG. 3. Normalized time-average current from the single electron capacitor model as a function of normalized electric field at cathode $E_c/E_{th}$ for a cylindrical diode of $R_c = 100$ nm, and gap spacing $D = R_a - R_c = 100$ nm. The dashed lines in the insert represent the time-average current of $I(t)$ (relative to the LB solution) for $E_c/E_{th} = 1.02$ at $N = 10$ and $E_c/E_{th} = 3$ at $N = 20$.

confirmed by Griswold *et al.* [20] in their particle-in-cell simulation.

The insets in Fig. 3 show the temporal evolution for the two cases, $E_c/E_{th} = 1.02$ at $N = 10$, and $E_c/E_{th} = 3$ at $N = 20$. Note that for $E_c/E_{th} = 1.02$, there is only one electron transported through the gap within one transit time, $T$ [cf. Eq. (5)]. The subsequent electron will only be injected into the gap while the prior electron nearly arrives at the anode. For $E_c/E_{th} = 3$, there is more than one electron (between 0.5 and 1.5) per transit time for which $I(t)$ is nonzero. Note that the inverse of the transit time shown in Fig. 3 corresponds to a frequency range of 0.1 to 1.5 THz for $D = 100$ nm from $E_c/E_{th} = 1.02$ to 4. The space charge effect will in general increase the vacuum transit time by 40% or more.

This Letter presents semiempirical formulas that provide an excellent approximation to the LB solutions for cylindrical and spherical diodes, essentially for the entire range of $R_c/R_a$ that is of practical significance. The dominant dependence is given by Eq. (7), which depends on the vacuum electric field on the cathode surface and is therefore quite different from the well-known Child-Langmuir's $V_g^{3/2}/D^2$ scaling given by Eq. (1). This simple dependence given in Eq. (7) was qualitatively derived by focusing on the approximate transit time of an electron sheet, which is spent mostly in the immediate vicinity of the cathode. This dominance of the vacuum field in the immediate vicinity of the cathode surface may have some implication in the contemporary development of electron gun codes, where modeling of electron emission in the first numerical grid proves most critical [30]. Corrections in the transit time from the effects of space charge are included, down to the Coulomb blockade regime where electrons numbered in the single digits are present in the diode.

The interesting connections between nano-particles, nano-cavities, Coulomb blockade, and the THz regime, remain to be explored. This model might be extended to the quantum regime [9,10,31], whose quantum CL law was recently used to study the charge transfer plasmons between two nearly touching metallic nanoparticles [32]. The proposed scaling might be useful to other space charge dominated systems, such as optical field emission at high field [33], organic semiconductors [34], metal-molecule-metal junction [35], nanowires [36], and a compact high power THz radiation source [37].

This work was supported by a Singapore MOE grant (No. 2008-T2-01-033), USA AFOSR AOARD grant (No. 11-4069), and USA ONRG grant (No. N62909-10-1-7135). A. V. would like to acknowledge the support of the Icelandic Research Fund Grant No. 120009021. P. Z. and Y. Y. L. were supported by an AFOSR grant on the Basic Physics of Distributed Plasma Discharges, and by AFOSR Grant No. FA9550-09-1-0662. They would also like to acknowledge discussions of this subject with Professor Richard Carter of the University of Lancaster, UK.

*ricky_ang@sutd.edu.sg

[1] C. D. Child, Phys. Rev. **32**, 492 (1911).
[2] I. Langmuir, Phys. Rev. **2**, 450 (1913).
[3] J. W. Luginsland, Y. Y. Lau, and R. M. Gilgenbach, Phys. Rev. Lett. **77**, 4668 (1996).
[4] Y. Y. Lau, Phys. Rev. Lett. **87**, 278301 (2001).
[5] R. J. Umstattd and J. W. Luginsland, Phys. Rev. Lett. **87**, 145002 (2001).
[6] J. W. Luginsland, Y. Y. Lau, R. J. Umstattd, and J. J. Watrous, Phys. Plasmas **9**, 2371 (2002).
[7] A. Rokhlenko and J. L. Lebowitz, Phys. Rev. Lett. **91**, 085002 (2003).
[8] W. S. Koh, L. K. Ang, and T. J. T. Kwan, Phys. Plasmas **12**, 053107 (2005).
[9] Y. Y. Lau, D. Chernin, D. G. Colombant, and P.-T. Ho, Phys. Rev. Lett. **66**, 1446 (1991).
[10] L. K. Ang, T. J. T. Kwan, and Y. Y. Lau, Phys. Rev. Lett. **91**, 208303 (2003).
[11] L. K. Ang, W. S. Koh, Y. Y. Lau, and T. J. T. Kwan, Phys. Plasmas **13**, 056701 (2006).
[12] S. Bhattacharjee, A. Vartak, and V. Mukherjee, Appl. Phys. Lett. **92**, 191503 (2008).
[13] K. L. Jensen, J. Lebowitz, Y. Y. Lau, and J. Luginsland, J. Appl. Phys. **111**, 054917 (2012).
[14] A. Valfells, D. W. Feldman, M. Virgo, P. G. O'Shea, and Y. Y. Lau, Phys. Plasmas **9**, 2377 (2002).
[15] L. K. Ang and P. Zhang, Phys. Rev. Lett. **98**, 164802 (2007).
[16] V. P. Gopinath, J. P. Verboncoeur, and C. K. Birdsall, Phys. Plasmas **3**, 2766 (1996).

[17] X. Chen, J. Dickens, L. L. Hattfield, E. H. Choi, and M. Kristiansen, Phys. Plasmas **11**, 3278 (2004).
[18] A. Pedersen, A. Manolescu, and A. Valfells, Phys. Rev. Lett. **104**, 175002 (2010).
[19] M. E. Griswold, N. J. Fisch, and J. S. Wurtele, Phys. Plasmas **17**, 114503 (2010).
[20] M. E. Griswold, N. J. Fisch, and J. S. Wurtele, Phys. Plasmas **19**, 024502 (2012).
[21] R. E. Caflisch and M. S. Rosin, Phys. Rev. E **85**, 056408 (2012).
[22] Y. Zhu and L. K. Ang, Appl. Phys. Lett. **98**, 051502 (2011).
[23] S. H. Chen, L. C. Tai, Y. L. Liu, L. K. Ang, and W. S. Koh, Phys. Plasmas **18**, 023105 (2011).
[24] R. J. Umstattd, C. G. Carr, C. L. Frenzen, J. W. Luginsland, and Y. Y. Lau, Am. J. Phys. **73**, 160 (2005).
[25] I. Langmuir and K. B. Blodgett, Phys. Rev. **22**, 347 (1923).
[26] I. Langmuir and K. B. Blodgett, Phys. Rev. **24**, 49 (1924).
[27] R. G. Carter (private communication).
[28] W. Shockley, J. Appl. Phys. **9**, 635 (1938).
[29] S. Ramo, Proc. IRE **27**, 584 (1939).
[30] J. Petillo, E. Nelson, J. Deford, N. Dionne, and B. Levush, IEEE Trans. Electron Devices **52**, 742 (2005).
[31] L. K. Ang, Phys. Rev. Lett. **109**, 219802 (2012).
[32] L. Wu, H. Q. Duan, P. Bai, M. Bosman, J. K. W. Yang, and E. P. Lee, ACS Nano **7**, 707 (2013).
[33] R. Bormann, M. Gulde, A. Weismann, S. V. Yalunin, and C. Ropers, Phys. Rev. Lett. **105**, 147601 (2010).
[34] A. Carbone, B. K. Kotowska, and D. Kotowski, Phys. Rev. Lett. **95**, 236601 (2005).
[35] J. M. Beebe, B. S. Kim, J. W. Gadzuk, C. D. Frisbie, and J. G. Kushmerick, Phys. Rev. Lett. **97**, 026801 (2006).
[36] A. A. Talin, F. Leonard, B. S. Swartzentruber, X. Wang, and S. D. Hersee, Phys. Rev. Lett. **101**, 076802 (2008).
[37] J. H. Booske, R. J. Dobbs, C. D. Joye, C. L. Kory, G. R. Neil, G.-S. Park, J. Park, and R. J. Temkin, IEEE Trans. Terahertz Sci. Technol. **1**, 54 (2011).